33rd Annual International Conference of the IEEE EMBS
Boston, Massachusetts USA, August 30 - September 3, 2011

High-Resolution MREIT using Low Imaging Currents

Eung Je Woo, *Senior Member, IEEE*

***Abstract*—Magnetic Resonance Electrical Impedance Tomography (MREIT) produces cross-sectional images of a conductivity distribution inside the human body. We use an MRI scanner as a tool to measure induced internal magnetic flux density distributions subject to externally injected currents. Recent experimental MREIT studies demonstrated conductivity image reconstructions of *in vivo* animal and human subjects with a few millimeter pixel size using 3 mA current injections. To enhance the clinical applicability of MREIT especially in neuroimaging applications, it is necessary to develop high-resolution MREIT techniques using low imaging currents. In this study, we demonstrate the capability of MREIT to perform conductivity imaging with less than 1 mA injection currents. The experimental results using a 3 T MRI scanner with a multi-echo ICNE pulse sequence and high-performance RF coils demonstrate that we can distinguish two different anomalies in reconstructed conductivity images with less than 1 mm pixel sizes. We plan to apply the developed experimental method to *in vivo* head imaging of small animals to investigate the feasibility of functional MREIT as a new neuro-imaging method.**

I. Introduction

Magnetic Resonance Electrical Impedance Tomography (MREIT) has been suggested as a new conductivity imaging modality [1,2] based on a current-injection MRI method [3]. The conductivity of a biological tissue is determined by its molecular composition, cellular structure, amounts of intra- and extra-cellular fluids, concentration and mobility of ions in those fluids, temperature and other factors [4,5]. As summarized in [6], it is also known that neural activities alter the conductivity directly and instantaneously.

Previous studies have demonstrated that conductivity image reconstructions with a pixel size of a few mm are possible by injecting a few mA currents [7,8]. In latest experimental studies, injection currents of about 3 mA were used to successfully produce conductivity images [9]. To enhance the clinical applicability of MREIT especially in head and chest imaging applications, we need to further reduce the amount of injection currents.

High-resolution MREIT is needed to distinguish fine structures inside human subjects and also in small animals. In this study, we conducted MREIT phantom experiments to reconstruct conductivity images with less than 1 mm pixel sizes. To compensate for the reduced SNR due to a small pixel size, we adopted a multi-echo ICNE pulse sequence [10-12] and high-performance small volume RF coils. After describing experimental methods, we will compare reconstructed conductivity images at various spatial resolutions.

E. J. Woo is with the Department of Biomedical Engineering, Kyung Hee University, Gyeonggi-do 446-701 KOREA (phone: +82-31-201-2538; fax: +82-31-201-2378; e-mail: ejwoo@ khu.ac.kr).

II. Methods

A. Phantom for High-Resolution MREIT

We used an octagon-shaped acrylic phantom. Its four long edges were 15 mm and the other four short edges were 10 mm. We installed four recessed carbon-hydrogel electrodes to inject currents. We placed two hollow cylindrical anomalies of thin insulating films (cellulose acetate, 0.3 mm thickness) with 5 mm diameter. On the side of one hollow cylinder, we made four equally-spaced holes along the central plane of the phantom where current-injection electrodes were located. We filled the background of the phantom including inside and outside of the two hollow cylinders with a saline of 0.12 S/m conductivity (0.3 g/l NaCl and 1 g/l $CuSO_4$).

B. Phantom for MREIT using Low Imaging Currents

We built an acrylic phantom of the thorax ($30\times14\times15$ cm^3) and breast (11 cm in diameter). Fig. 1(a) shows the picture of the breast phantom. After filling the phantom with a saline of 0.12 S/m conductivity (0.3 g/l NaCl and 1 g/l $CuSO_4$), two different biological tissues of porcine muscle and chicken breast were positioned in the phantom. Their conductivity values were 0.64 and 0.60 S/m. We attached four carbon-hydrogel electrodes around the breast area of the phantom. We injected currents using the electrode configuration shown in Fig. 1(b) [1,13].

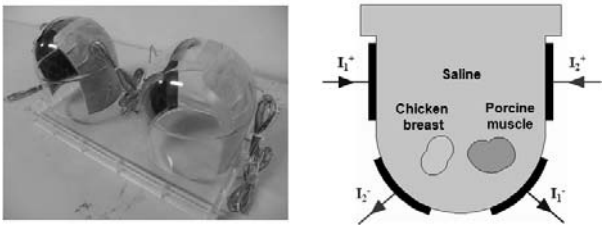

(a) (b)

Fig. 1. (a) Breast phantom and (b) electrode configuration for imaging experiment with low injection currents.

C. Imaging Experiment

We placed the phantom inside the bore of a 3 T clinical MRI scanner (Siemens Medical Solutions, Erlangen, Germany) and performed MREIT scans. Using a custom-designed MREIT current source, we injected the first

current I_1 between one pair of electrodes. We changed the injection current amplitude from 3 mA down to 500 μA with the total pulse width of 28 ms. The multi-echo ICNE pulse sequence was used with TR/TE = 800/20 ms, FOV = 180×180 mm^2 and 55×55 mm^2, slice thickness = 4 mm, NEX = 8, matrix size = 128×128, number of slices = 7, and total imaging time = 40 min. After acquiring the first magnetic flux density (B_z) data set for I_1, the second injection current I_2 with the same amplitude and pulse width was injected through the other pair of electrodes to obtain the second data set.

D. Conductivity Image Reconstructions

We used CoReHA (Conductivity Image Reconstructor using Harmonic Algorithms) to produce conductivity images [14,15]. It provides GUI-based functions for all data processing routines needed to produce conductivity images from measured k-space data sets. We used the single-step harmonic B_z algorithm implemented in CoReHA for multi-slice conductivity image reconstructions [16]. All conductivity images presented in this paper should be interpreted as scaled conductivity images providing only contrast information.

III. RESULTS

A. High-Resolution MREIT

Fig. 2(a), (b) and (c) show an MR magnitude, magnetic flux density, and reconstructed conductivity images, respectively, of the phantom with two cylindrical anomalies. The pixel size of the images in Fig. 2 was 400 μm. From the reconstructed conductivity image in Fig. 2(c), we can see that the anomaly on the left (with four holes) shows a different conductivity contrast compared with the one on the right (without holes). Such a contrast was not seen in the magnitude image in Fig. 2(a). Note that the anomaly on the right appears to be an insulator since we are producing the conductivity image at a low frequency in MREIT.

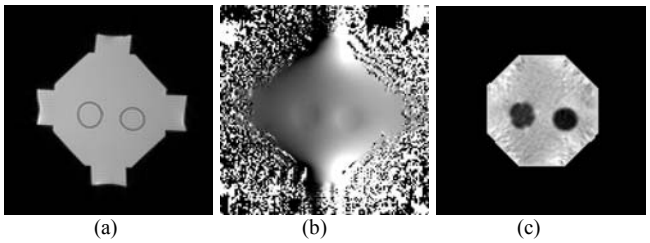

Fig. 2. (a) MR magnitude, (b) magnetic flux density, and (c) reconstructed conductivity images of the phantom with a 400 μm pixel size.

Fig. 3(a) and (b) show reconstructed conductivity images at spatial resolutions of 1.4 and 1 mm, respectively. The conductivity images in (c) and (d) were reconstructed from a second octagonal phantom with two anomalies at spatial resolutions of 400 and 200 μm, respectively. All the conductivity images except the one with 200 μm pixel size showed clear contrast between two different anomalies. The conductivity image with 200 μm pixel size was too noisy compared with other three cases primarily due to a poor SNR in measured data.

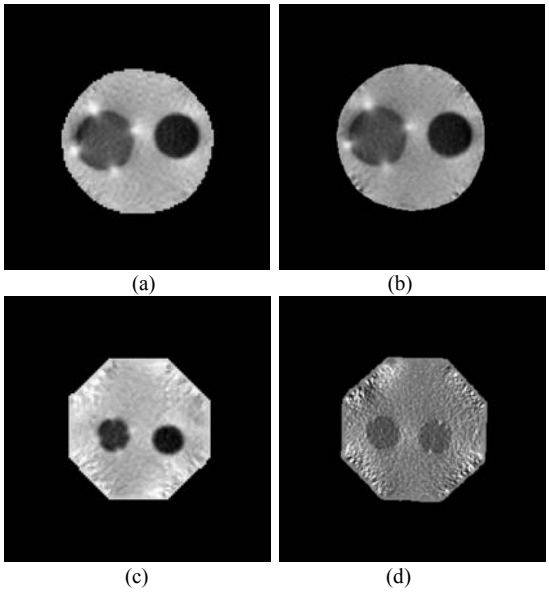

Fig. 3. Reconstructed conductivity images of two different anomalies at different spatial resolutions: (a) 1.4 mm, (b) 1 mm, (c) 400 μm and (d) 200 μm.

B. Low Imaging Current

Fig. 4(a), (b) and (c) show MR magnitude, magnetic flux density, and reconstructed conductivity images of the breast phantom with 3 mA current injections, respectively. Carbon-hydrogel electrodes with a large surface area and the multi-channel transmit/receive breast coil improved SNRs in measured magnetic flux density images. Two different tissues on the left and right sides show their conductivity contrasts in Fig. 4(c), whereas the MR magnitude image in Fig. 4(a) does not distinguish them.

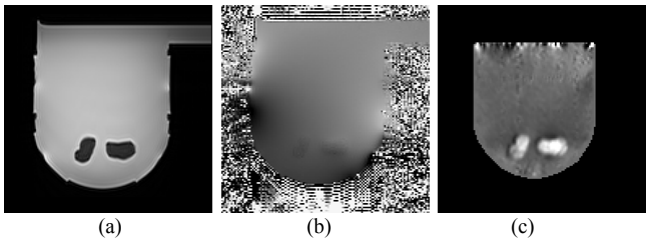

Fig. 4. (a) MR magnitude image, (b) magnetic flux density image, and (c) reconstructed conductivity image of the first breast phantom with 3 mA current injection.

Fig. 5 shows an MR magnitude of a different breast phantom in (a) and reconstructed conductivity images in (b)-(e) with 3, 1, 0.7, and 0.5 mA current injections, respectively. All the conductivity images except the case of

0.5 mA current injection show clear contrast between two different tissues. The conductivity image with 0.7 mA current injections is noisy but still distinguishes two tissues.

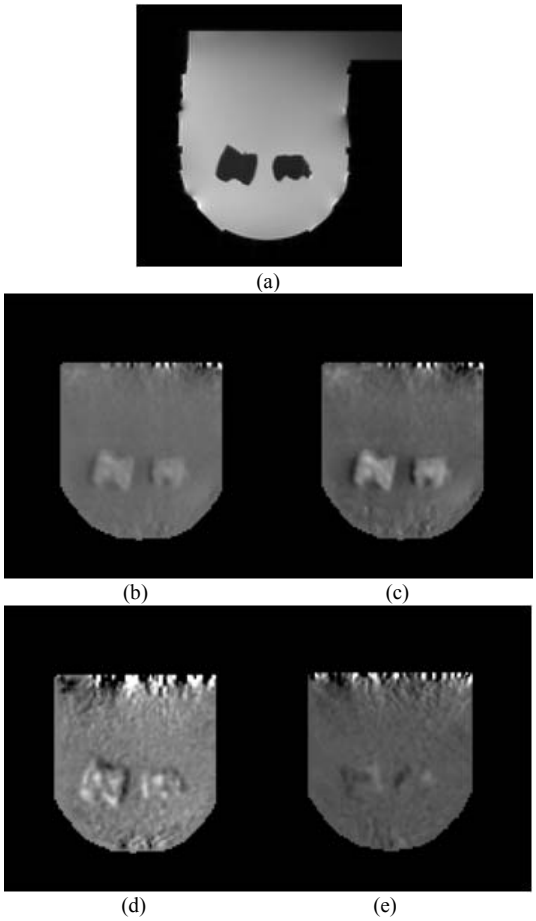

Fig. 5. (a) MR magnitude image of the second breast phantom. (b)-(e) are reconstructed conductivity images with 3, 1, 0.7 and 0.5 mA current injections, respectively.

IV. Discussion

The results demonstrate that the existing MREIT technique can produce conductivity images with a spatial resolution of as low as 400 μm. Using the multi-echo pulse sequence and high-performance small volume RF coils, we could achieve this spatial resolution with imaging currents of 3 mA.

Note that current entered the hollow insulating cylinder with four holes and produced ion conduction through the hollow cylinder. This increased the apparent conductivity of the hollow cylinder with four holes to distinguish itself from the other one without any hole [17]. The results clearly indicate that the reconstructed apparent conductivity is affected by ion mobility as well as ion concentration. We plan to try conductivity image reconstructions of hollow cylindrical anomalies of thin insulating film with various hole configurations to investigate contrast mechanism in MREIT. We will also adopt this kind of phantom design as a macroscopic model of conductivity change during neural activity.

Compared with other breast imaging techniques, a conductivity imaging method may better differentiate cancerous tissues in the breast since their conductivity values are several times higher than those of normal breast tissues [18]. In this study, we performed breast phantom MREIT imaging experiments using a multi-channel breast coil and current injections as small as 0.5 mA. To distinguish two tissues of 0.64, and 0.60 S/m conductivity values, we found that the injection current amplitude should be at least 0.7 mA.

To distinguish cancerous breast tissues with significantly larger conductivity values compared with normal tissues, we speculate that breast MREIT using less than 1 mA injection currents is feasible. We may further reduce the amplitude of injection currents by incorporating specialized breast coils and improved pulse sequences.

There will be technical issues not addressed in this paper related with MREIT scans of a real human head or chest. MR signals from the brain tissues will be smaller than the MR signals from the saline. The skull will block some amount of injected current to reduce current density values inside the brain thereby producing smaller magnetic flux density signals inside the brain. Based on the results in this study, we plan to optimize the electrode configuration to produce more uniform current distributions inside the imaging domain for better SNRs in measured magnetic flux density images.

Latest technical developments in MREIT show that a high-performance clinical 3 T MRI scanner with multiple high-sensitivity RF coils and optimized pulse sequences can provide more than 10 times improvements in the SNR of magnetic flux density measurements. We anticipate that high-resolution MREIT imaging of *in vivo* human and animal subjects will be feasible with less than 1 mA injection currents. We plan to undertake *in vivo* head imaging experiments of small animals using the experimental setup developed in this paper.

In the IEC60601-1 electrical safety standard, the patient auxiliary current is defined as current flowing in the patient in normal use between any patient connection and all other patient connections and not intended to produce a physiological effect. IEC60601-1 describes general safety standards for medical equipment. For certain medical equipment which needs more specific standards, IEC provides a separate document.

IEC60601-2-10 describes safety limits for nerve and muscle stimulators. The maximum current on a 500 Ω load is limited as follows: 80 mA_{rms} for dc, 50 mA_{rms} from dc to 400 Hz, 80 mA_{rms} from 400 Hz to 1.5 kHz, and 100 mA_{rms} above 1.5 kHz. For a pulse with its width of less than 0.1 s, power is limited by 300 mJ/pulse on 500 Ω load. Voltage must be less than 500 V.

We should interpret the patient auxiliary current in IEC60601-1 as the current flowing through a patient from medical equipment, which does not intentionally inject current into the patient. When we intentionally inject current

into a patient for diagnostic and/or therapeutic purposes, there must be a separate safety standard or the manufacturer must provide enough rationale for using such injection currents and clinical significance of the equipment. It is, therefore, inappropriate to link the patient auxiliary current in IEC60601-1 as the maximum allowed injection current in MREIT.

We should note that previous studies showed that 1 A/m^2 current density below 1 kHz can stimulate a nerve of 20 μm diameter. Injecting 2.5 mA through a $5\times5cm^2$ electrode will produce 1 A/m^2 current density if we use a uniform current density electrode. Considering these, we speculate that MREIT scans using 1 mA injection currents, for example, may find clinical applications.

V. Conclusion

We found that MREIT using a high-performance clinical 3 T MRI scanner has a potential as a high-resolution conductivity imaging method using less than 1 mA injection currents. We suggest future studies of SNR improvements through better pulse sequence designs, multiple high-sensitivity RF coils, better algorithms for denosing and image reconstructions, and also statistical time-series analyses of functional MREIT images. Numerical simulations as well as tissue phantom experiments such as [19,20] are needed to better understand and quantify conductivity contrast.

Acknowledgment

This work was supported by the National Research Foundation of Korea (NRF) grant funded by the Korea government (MEST) (No. 20100018275).

References

[1] E. J. Woo and J. K. Seo, "Magnetic resonance electrical impedance tomography (MREIT) for high-resolution conductivity imaging," Physiol. Meas., vol. 29, pp. R1-R26, 2008.

[2] J. K. Seo and E. J. Woo, "Magnetic resonance electrical impedance tomography (MREIT)," SIAM Rev., vol. 52, pp. 40-68, 2011.

[3] G. C. Scott, M. L. G. Joy, R. L. Armstrong and R. M. Henkelman, "Measurement of nonuniform current density by magnetic resonance," IEEE Trans. Med. Imag., vol. 10, pp. 362-374, 1991.

[4] S. Gabriel, R. W. Lau and C. Gabriel, "The dielectric properties of biological tissues: II. measurements in the frequency range 10 Hz to 20 GHz," Phys. Med. Biol., vol. 41, pp. 2251-2269, 1996.

[5] S. Grimnes and O. G. Martinsen, Bioimpedance and Bioelectricity Basics, 2nd ed., Academic Press, Oxford, UK, 2008.

[6] D. Holder and T. Tidswell, "Electrical impedance tomography of brain function," in D. Holder, Electrical Impedance Tomography: Methods, History and Applications, IOP Publishing, Bristol, UK, 2005.

[7] H. J. Kim, B. I. Lee, Y. Cho, Y. T. Kim, B. T. Kang, H. M. Park, S. Y. Lee, J. K. Seo, and E. J. Woo, "Conductivity imaging of canine brain using a 3 T MREIT system: postmortem experiments", Physiol. Meas., vol. 28, pp. 1341-1353, 2007.

[8] H.J. Kim, T.I. Oh, Y.T. Kim, B.I. Lee, E.J. Woo, J.K. Seo, S.Y. Lee, O. Kwon, C. Park, B.T. Kang, and H.M. Park, "In vivo electrical conductivity imaging of a canine brain using a 3T MREIT system", Physiol. Meas., vol. 29, pp. 1145-1155, 2008.

[9] H. J. Kim, Y. T. Kim, A. T. Minhas, Z. Meng, and E. J. Woo, "Breast MREIT phantom experiments using less than 1 mA injection currents," Proc. Int. Conf. EIT, Bath, UK, 2011.

[10] D. A. Feinberg, C. M. Mills, J. P. Posin, D. A. Ortendahl, N. M. Hylton, L. E. Crooks, J. C. Watts, L. Kaufman, M. Arakawa, J. C. Hoenninger and M Brant-Zwadwaski, "Multiple spin-echo magnetic resonance imaging", Radiology, vol. 155, pp. 437-442, 1985.

[11] C. Park, B. I. Lee, O. Kwon, and E. J. Woo, "Measurement of induced magnetic flux density using injection current nonlinear encoding (ICNE) in MREIT," Physiol. Meas., vol. 28, pp. 117-127, 2006.

[12] A. S. Minhas, W. C. Jeong, Y. T. Kim, Y. Q. Han, H. J. Kim, E. J. Woo, "Experimental performance evaluation of multi-echo ICNE pulse sequence in MREIT", Magn. Reson. Med., at press, 2011.

[13] B. I. Lee, S. H. Oh, T. S. Kim, E. J. Woo, S. Y. Lee, O. Kwon, J. K. Seo, "Basic setup for breast conductivity imaging using magnetic resonance electrical impedance tomography", Phys. Med. Biol., vol. 51, pp. 443-455, 2006.

[14] K. Jeon, A. S. Minhas, Y. T. Kim, W. C. Jeong, H. J. Kim, B. T. Kang, H. M. Park, C. O. Lee, J. K. Seo and E. J. Woo, " MREIT conductivity imaging of postmortem canine abdomen using CoReHA", Physiol. Meas., vol. 30, pp. 957-966, 2009.

[15] K. Jeon, H. J. Kim, C. O. Lee, E. J. Woo, J. K. Seo, "CoReHA: conductivity reconstructor using harmonic algorithms for magnetic resonance electrical impedance tomography (MREIT)", J. Biomed. Eng. Res., vol. 30, pp. 279-287, 2009.

[16] J. K. Seo, S. W. Kim, S. Kim, J. J. Liu, E. J. Woo, K. Jeon, C. O. Lee, "Local harmonic Bz algorithm with domain decomposition in MREIT: computer simulation study", IEEE Trans. Med. Imag., vol. 27, pp. 1754-1761, 2008.

[17] T. I. Oh, Y. T. Kim, A. Minhas, J. K. Seo, O. I. Kwon, and E. J. Woo, "Ion mobility imaging and contrast mechanism of apparent conductivity in MREIT," Phys. Med. Biol., vol. 56, pp. 2265-2277, 2011.

[18] L. T. Muftuler, M. J. Hamamura, O. Birgul and O. Nalcioglu, "In vivo MRI electrical impedance tomography (MREIT) of tumors", Technol. Cancer. Res. Treat., vol. 5, pp. 381-387, 2006.

[19] A. S. Minhas, Z. Meng, Y. T. Kim, H. J. Kim, E. J. Woo, and H. H. Kim, "Three-dimensional MREIT simulator (MREITSim)," Proc. NFSI & ICBEM, Banff, Canada, 2011.

[20] R. J. Sadleir, S. C. Grant and E. J. Woo, "Can high-field MREIT be used to directly detect neural activity? Theoretical considerations," NeuroImage, vol. 52, pp. 205-216, 2010.